Substrate–Cofactor Interactions for Glycogen Phosphorylase *b*: A Binding Study in the Crystal with Heptenitol and Heptulose 2-Phosphate†

P. J. McLaughlin, D. I. Stuart, H. W. Klein, N. G. Oikonomakos,‡ and L. N. Johnson*

ABSTRACT: The structural relationships between substrate and pyridoxal phosphate in glycogen phosphorylase *b* (EC 2.4.1.1) have been studied by X-ray diffraction experiments at 3-Å resolution. Recent work [Klein, H. W., Im, M. J., & Helmreich, E. J. M. (1984) in *Chemical and Biological Aspects of Vitamin B_6 Catalysis* (Evangelopoulos, A. E., Ed.) pp 147–160, Liss, New York] has shown that phosphorylase in the presence of inorganic phosphate catalyzes the conversion of heptenitol to heptulose 2-phosphate. The latter compound is a dead-end product and a most potent inhibitor (K_i = 14 μM). The X-ray diffraction studies show that heptenitol binds at the catalytic site of phosphorylase in a position essentially identical with that observed for the glucopyranose moiety of glucose 1-phosphate. Incubation of a phosphorylase *b* crystal for 50 h in a solution containing the substrates heptenitol and inorganic phosphate and the activators AMP and maltohetaose resulted in the formation of a phosphorylated product bound at the active site. The structure of this product, as analyzed by a difference Fourier synthesis at 3 Å, is consistent with that of heptulose 2-phosphate. Analysis of the surrounding soak solution by thin-layer chromatography showed that heptulose 2-phosphate was produced under these conditions. Heptulose 2-phosphate binds with its glucopyranose moiety in the same position as that for glucose 1-phosphate, but there is a marked difference in phosphate positions. The presence of the methyl group in the β-configuration in heptulose 2-phosphate forces a change in the torsion angle O5–C1–O1–P from 117° as observe in glucose 1-phosphate to −136° in heptulose 2-phosphate. The "down" position of the phosphate (with respect to the crystallographic *z* axis) results in a change in the distance between the 5′-phosphorus atom of the pyridoxal phosphate and the phosphorus atom of the substrate from 6.8 (with glucose 1-phosphate) to 4.5 Å (with heptulose 2-phosphate). The closest distance between the phosphate oxygen of the cofactor and a phosphate oxygen of heptulose 2-phosphate is 2.7 Å, and it is assumed that there must be a hydrogen bond between them. These observations are consistent with the NMR experiments reported in the preceding paper in which sharing of a proton between heptulose 2-phosphate and pyridoxal 5′-phosphate is observed [Klein, H. W., Im, M. J., Palm, D., & Helmreich, E. J. M. (1984) *Biochemistry* (preceding paper in this issue)]. The crystallographic results are discussed in light of current proposals for the role in catalysis of the 5′-phosphate of the cofactor. It is argued that the down position observed for the phosphate of heptulose 2-phosphate is likely to be the position occupied during catalysis. When the substrate phosphate is in this position, the cofactor phosphate can participate directly in catalysis, most likely as an acid–base but possibly as an electrophile. The down position of the phosphate allows greater scope for aproach of the oligosaccharide substrate and interconversion of the ternary enzyme–substrate complex.

Glycogen phosphorylase (EC 2.4.1.1) catalyzes the reversible phosphorylation of the α(1–4) glycosidic linkage from the nonreducing ends of glycogen. The mechanism by which the enzyme uses its essential cofactor, pyridoxal phosphate, in this reaction has long been a mystery. Reconstitution studies of the apoenzyme with modified cofactors and ^{31}P NMR[1] experiments have established that the 5′-phosphate group is essential for activity [see reviews by Graves & Wang (1972), Parrish et al (1977), and Helmreich & Klein (1980)]. The structural studies on both phosphorylase *a* (Sprang & Fletterick, 1979) and phosphorylase *b* (Weber et al., 1978) have demonstrated the proximity of the pyridoxal phosphate to the substrate binding site of this large enzyme.

Recent X-ray crystallographic experiments and further ^{31}P NMR measurements and reconstitution studies with cofactor and substrate analogues have shown that the substrate phosphate and 5′-phosphate of the cofactor are in close proximity in the enzyme–substrate complex (Johnson et al., 1980; Jenkins et al., 1981; Withers et al., 1982a,b, 1981a,b; Klein et al., 1982, 1984a,b; Takagi et al., 1982; Madsen & Withers, 1984; Shimomura & Fukui, 1980; Fukui et al., 1984). However, several different mechanisms have been proposed for the role of the 5′-phosphate group: as a nucleophile or electrostatic stabilizing group (Johnson et al., 1980); as an acid–base catalyst (Feldman et al., 1978; Helmreich & Klein, 1980; Klein et al., 1982); with the phosphorus atom as an electrophile (Withers et al., 1981b, 1982a; Takagi et al., 1982). It is therefore of interest to establish as precisely as possible the disposition of the two phosphate groups in the enzyme–substrate complex.

Crystallographic studies with phosphorylase *b* have shown that the phosphorus–phosphorus distance when glucose 1-phosphate (K_m = 37 mM) is bound is 6.5 Å but that with the more strongly binding competitive inhibitor glucose cyclic 1,2-phosphate (K_i = 500 μM) the phosphorus–phosphorus distance is only 5.3 Å. In this case, the phosphate oxygens

† From the Laboratory of Molecular Biophysics, Zoology Department, Oxford OX1 3PS, England (P.J.M., D.I.S., N.G.O., and L.N.J.), and the Department of Physiological Chemistry, The University of Würzburg, School of Medicine, D-8700 Würzburg, Federal Republic of Germany (H.W.K.). *Received February 3, 1984.* This work was supported by grants from Science and Engineering Research Council and the Medical Research Council. P.J.M. was supported by a Northern Ireland postgraduate studentship. N.G.O. was supported by fellowships from the British Council and the Federation of European Biochemical Societies.

‡ On leave from the Biochemistry Department, Centre for Biological Research, National Hellenic Research Foundation, Athens, Greece.

[1] Abbreviations: heptenitol, 2,6-anhydro-1-deoxy-D-*gluco*-hept-1-enitol; heptulose 2-phosphate, 1-deoxy-D-*gluco*-heptulose 2-phosphate; glucose 1-phosphate, α-D-glucopyranose 1-phosphate; glucose cyclic 1,2-phosphate, α-D-glucopyranose cyclic 1,2-phosphate; AMP, adenosine 5′-monophosphate; BES, *N*,*N*-bis(2-hydroxyethyl)-2-aminoethanesulfonic acid; EDTA, ethylenediaminetetraacetic acid; IMP, inosine 5′-monophosphate; NMR, nuclear magnetic resonance. The nomenclature used to describe the atoms of amino acid residues follows that of the Protein Data Bank (Bernstein et al., 1977); this nomenclature is similar to that of the IUPAC–IUB convention except that Roman characters replace the Greek letters.

0006-2960/84/0423-5862$01.50/0

Chart I

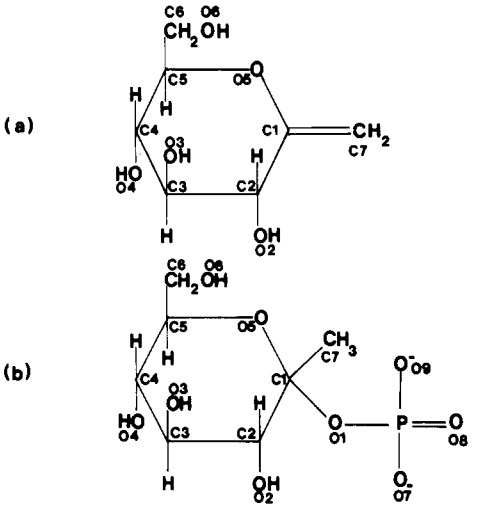

are sufficiently close to allow (if not to require) a hydrogen bond between them (Johnson et al., 1980; Jenkins et al., 1981; Sansom et al., 1984). These binding studies were carried out with crystals of a partially activated form of the enzyme that are obtained in the presence of 2 mM IMP. IMP is a weak activator: it promotes activity but without bringing about the concomitant increase in affinity for substrate that is observed in the presence of the strong activator AMP (Black & Wang, 1968). A difficulty arose, however, in attempting to extrapolate from these substrate (inhibitor) binding studies to a mechanism. No binding at the active site of the second substrate, glycogen, was observed in the crystal. Examination of the molecular model showed that a substantial movement of the protein and/or a distortion of the substrate from the preferred conformation of $\alpha(1\text{–}4)$-linked oligosaccharides was required before glycogen analogues could bind. Hence, until direct observations on the ternary enzyme–substrate complex are possible, there is some doubt as to the nature of the productive enzyme–substrate complex.

In the preceding paper and previously, Klein et al. (1984a,b) have described heptenitol as a substrate for phosphorylase. In the presence of inorganic phosphate, phosphorylase converts heptenitol to heptulose 2-phosphate in a reaction that does not require oligo- or polysaccharide. Heptulose 2-phosphate is a dead-end product and inhibits the phosphorylase reaction with a K_i = 14 μM, making it the tightest of all inhibitors known for phosphorylase. This reaction is an attractive system for study in the crystal because it does not require oligosaccharide substrate and because it leads to a high-affinity product that may resemble the transition state of the natural reaction. In this paper, we report on the binding of heptenitol to phosphorylase at 3-Å resolution. We have also used a crystal of phosphorylase *b* soaked in a mixture of heptenitol and phosphate in the presence of activators AMP and oligosaccharide to synthesise heptulose 2-phosphate. The binding of the latter compound has been studied with the aid of the intense synchrotron radiation source at the Science and Engineering Research Council's Laboratory at Daresbury.

The numbering system for the atoms of heptenitol and heptulose 2-phosphate is shown in Chart I. We prefer this system to that of conventional carbohydrate chemistry because it allows direct comparison with our previous results for glucose 1-phosphate and glucose cyclic 1,2-phosphate.

Materials and Methods

Rabbit muscle phosphorylase *b* was prepared by the method of Fischer & Krebs (1962), with minor modifications. Crystals were grown from a solution of 25–30 mg/mL phosphorylase *b*, 2 mM IMP, 10 mM BES, 10 mM magnesium acetate, 3 mM dithiothreitol, and 0.1 mM EDTA, pH 6.7 (Johnson et al., 1974). The crystals are tetragonal, space group $P4_32_12$ with unit-cell dimensions $a = b = 128.6$ Å and $c = 116.6$ Å. The crystallographic asymmetric unit contains one subunit of the enzyme (M_r 97 412), and the two subunits of the physiologically active dimer are related by the crystallographic two-fold axis at $z = 0.5$.

Heptenitol was synthesised as described in the preceding paper (Klein et al., 1984b) following the method of Hehre et al. (1980). Maltoheptaose was a gift from Boehringer Co., Mannheim, Germany. Other chemicals were obtained from Sigma Chemical Co.

Soaking Conditions and Data Collection. (*a*) *Heptenitol.* Crystals were soaked for 18 h already mounted in thin-walled glass capillary tubes in 100 mM heptenitol, 10 mM BES, 10 mM magnesium acetate, and 0.1 mM EDTA, pH 6.7. Data to 3-Å resolution were recorded with an Arndt-Wonacott oscillation camera using Ni-filtered Cu Kα radiation from an Elliott GX6 rotating anode X-ray generator run at 40 kV, 40 mA. The crystal to film distance and collimator aperture size were 100 mm and 0.6 mm, respectively. The crystal was oscillated about the *c* axis with oscillation range ($\Delta\phi$) 1.5° per film with a speed of 7.5×10^3 s deg^{-1}. Data collection for the total range of ϕ = 0–45° required two crystals and took 1 week. The data, after reduction to a unique data set, represented over 85% of the total data to 3-Å resolution.

(*b*) *Heptulose 2-Phosphate.* Because heptulose 2-phosphate is not readily available, it was synthesised in situ from heptenitol and phosphate by using phosphorylase crystals. Crystals, extensively washed and already mounted for diffraction studies in thin-walled glass capillaries, were soaked in a solution containing 100 mM heptenitol, 50 mM $NaH_2PO_4 \cdot 2H_2O$, 50 mM maltoheptaose, 2.5 mM AMP, 10 mM BES, 10 mM magnesium acetate, and 0.1 mM EDTA, pH 7.0, for 50 h at 23 °C. Oligosaccharide was included as activator in the soaking mixture because the rabbit muscle enzyme (in contrast to the potato enzyme) requires occupation of the glycogen storage site for the heptenitol reaction. AMP (and not IMP) was added to the soaking solution in order to facilitate activation of phosphorylase *b* to its high-affinity state (Black & Wang, 1968). The concentration of AMP (2.5 mM) was adjusted so as to optimize occupation of the allosteric effector site without occupation of the nucleoside inhibitor site. [The K_i values for AMP and IMP binding to the nucleoside inhibitor site are 6.0 mM and 1.5 mM, respectively (Kasvinsky et al., 1978).] During soaking, large cracks perpendicular to the *c* axis appeared in the crystals.

Data to 3-Å resolution were collected at the Science and Engineering Research Council's Synchrotron Radiation Source at Daresbury, Warrington. The storage ring was operated at 2 GeV, 150 mA, multibunch mode. The X-ray beam was focused in the vertical direction by a bent quartz mirror and focused in the horizontal direction and monochromated by a germanium curved triangular crystal with the (111) planes cut at an angle to the surface (Helliwell et al., 1982). The wavelength was 1.488 Å. A similar procedure for data collection as that described for the heptenitol experiment was used but with a 100-fold reduction in exposure time (speed 75 s deg^{-1}). The data were collected in 2.5 h. After reduction to the unique data set, these measurements represent 94% of the total data to 3-Å resolution.

Data Processing and Interpretation. The X-ray films were digitized on a Scandig 3 microdensitometer with a 100-μm spot and raster. Integrations were carried out on a PDP11/70 computer with a version of the MOSCO suite of programs (Stuart et al., 1979; Wilson et al., 1983), which had been further modified for profile fitting of the spot shape. Subsequent data processing was carried out as described by Wilson & Yeates (1979), and the data were scaled to the master 2-Å native data set (Wilson et al., 1983).

The crystal structure of phosphorylase *b* has been refined at 2-Å resolution by the method of restrained least-square crystallographic refinement (Konnert, 1976; Hendrickson & Konnert, 1980). At the present stage in the analysis, the crystallographic *R* value for some 52 329 reflections in the 5–2-Å resolution range is 0.37. The root mean square deviation from ideal bond lengths for some 6640 atoms is 0.019 Å. The refinement has some way to go before completion, but analysis suggests that about 75% of the structure is correct. Careful examination of the native electron density map based on improved phases has shown several corrections to the structure since our last publication (Sansom et al., 1984). The changes that are important for the discussion in this paper are (i) a refitting of residues Asn-337 and Asp-338 so that Asp-338 makes an internal hydrogen bond to His-376 but is not involved in the substrate binding site, (ii) a rearrangement of residues 570–574, which results in His-570 pointing away from and Tyr-572 pointing toward the catalytic site, and (iii) a rearrangement of residues 283–284 to allow better use of the density and which results in Asn-284 pointing into the catalytic site and an interaction of Asp-283 with Arg-568, as observed for phosphorylase *a* (Sprang et al., 1982).

Difference Fourier syntheses were computed by using the phases obtained from a combination of those determined by isomorphous replacement techniques and those calculated during the crystallographic refinement for the 5–3-Å resolution range (mean figure of merit 0.78) and the isomorphous phases for the ∞–5-Å resolution range (mean figure of merit 0.85). The coefficients for the difference Fourier syntheses were $F_{Hept} - F_p$, $F_{H2P} - F_p$, and $F_{H2P} - F_{Hept}$, where F_p, and F_{Hept}, and F_{H2p} are the structure factor amplitudes for the native, the heptenitol complex, and the heptulose 2-phosphate–AMP–maltoheptaose complex, respectively.

Binding sites were located on small-scale difference maps of the complete asymmetric unit (scale 2 mm/Å) and examined in detail with the program FRODO (Jones, 1978, 1982) implemented on an Evans and Sutherland Picture System II /PDP 11/70 computer. The coordinates for the "averaged" glucopyranose ring (Arnott & Scott, 1972) were used to fit the glucose moieties. Atoms were considered to be in van der Waals contact with those of the protein if their separations were less than 4.5 Å. Possible hydrogen bonds were noted if the distance between donor and acceptor was less than 3.5 Å and if the bond was linear to within 40°. These rather generous limits reflect the present accuracy of our model.

Heptenitol Reaction in Crystals. Thin-layer chromatography was performed on silica gel 60 F-250 plates from Merck in a solvent system of ethanol/propan-2-ol/ammonia/water (7:1:1:2). Sugar and phosphate were stained with phosphomolybdic acid (3% in ethanol). R_f values for glucose 1-phosphate, heptulose 2-phosphate, heptenitol, heptitol, and maltoheptaose were found from control experiments with purified compounds.

Three crystals (approximate size 1 mm × 0.3 mm × 0.3 mm) were carefully washed with five changes of 10 mM BES, 10 mM magnesium acetate, and 0.1 mM EDTA buffer, pH 7.0. Each crystal was placed in a small test tube containing 50 μL of 100 mM heptenitol, 50 mM $NaH_2PO_4 \cdot 2H_2O$, 50 mM maltoheptaose, 2.5 mM AMP, 10 mM BES, 10 mM magnesium acetate, and 0.1 mM EDTA, pH 7.0 (solution A, i.e., a solution of identical composition to that used in the X-ray experiment). Incubations were carried out at 25 °C. Aliquots (approximately 2 μL) were removed after 10 min, 1 h, 24 h, and 50 h and analyzed by thin-layer chromatography. Two control experiments were run in parallel. In the first, the crystal was omitted in order to detect the stability of the compounds without enzyme, and in the second, the maltoheptaose was omitted in order to test the activating properties of the oligosaccharide.

A second experiment was carried out to determine whether the surrounding soak solution of the crystal after 50-h incubation contained sufficient enzyme molecules to bring about catalysis. Three crystals were washed and soaked in solution A except that the substrate, heptenitol, was omitted. A total of 10 μL of the soak solution was removed after 50 h, and reaction was started by mixing this with an equal volume of solution A in which the heptenitol was 200 mM. Incubations were continued for a further 50 h and aliquots analyzed by thin-layer chromatography. Three control experiments were carried through: in the first, the crystal was omitted from the soak solution; in the second, maltoheptaose was omitted throughout; and in the third, heptenitol was omitted throughout in order to detect reaction of oligosaccharide and phosphate to form glucose 1-phosphate.

Table I: Summary of Data Processing Statistics for Phosphorylase *b* Complexes

complex	resolution (Å)	total reflections measured	no. of independent reflections	merging R^a	fractional change in *F*
heptenitol	3	73 677	16 041	0.066	0.103
heptulose-2-P–AMP–maltoheptaose	3	88 108	18 715	0.063	0.145

$^a R = \sum_i \sum_h |\bar{I}(h) - I_i(h)| / [\sum_i \sum_h I_i(h)]$, where $I_i(h)$ is the *i*th measurement of the intensity of reflection *h* and $\bar{I}(h)$ is the mean of these measurements.

Results

Data Collection. A summary of the three-dimensional data processing statistics is given in Table I. The statistics are especially good for the heptulose 2-phosphate complex. These crystals were cracked, but use of the finely collimated, nondivergent, synchrotron radiation beam allowed data to be recorded by shooting between the cracks. Radiation damage, which is always more severe in cracked crystals, was alleviated by the presence of oligosaccharide in the crystals (Stura, 1981) and the use of the brilliant source. Radiation damage is not simply related to total dose, and experience [e.g., Wilson et al., (1983)] suggests that for phosphorylase crystals a high dose for a short time is less damaging than a low dose for a long time. In this instance, the short data collection time (2.5 h) with synchrotron radiation made possible an experiment that would have been extremely difficult with a conventional source.

The Binding Sites. A general description of the phosphorylase *b* molecule has been given in previous publications (Weber et al., 1978; Johnson et al., 1980; Jenkins et al., 1981; Stura et al., 1983; Sansom et al., 1984). The results, with an explanation of the nomenclature, are summarized in Figure 1. The catalytic site (site C), identified from the binding of the substrate glucose 1-phosphate, is situated at the center of the molecule where the structural domains come together and

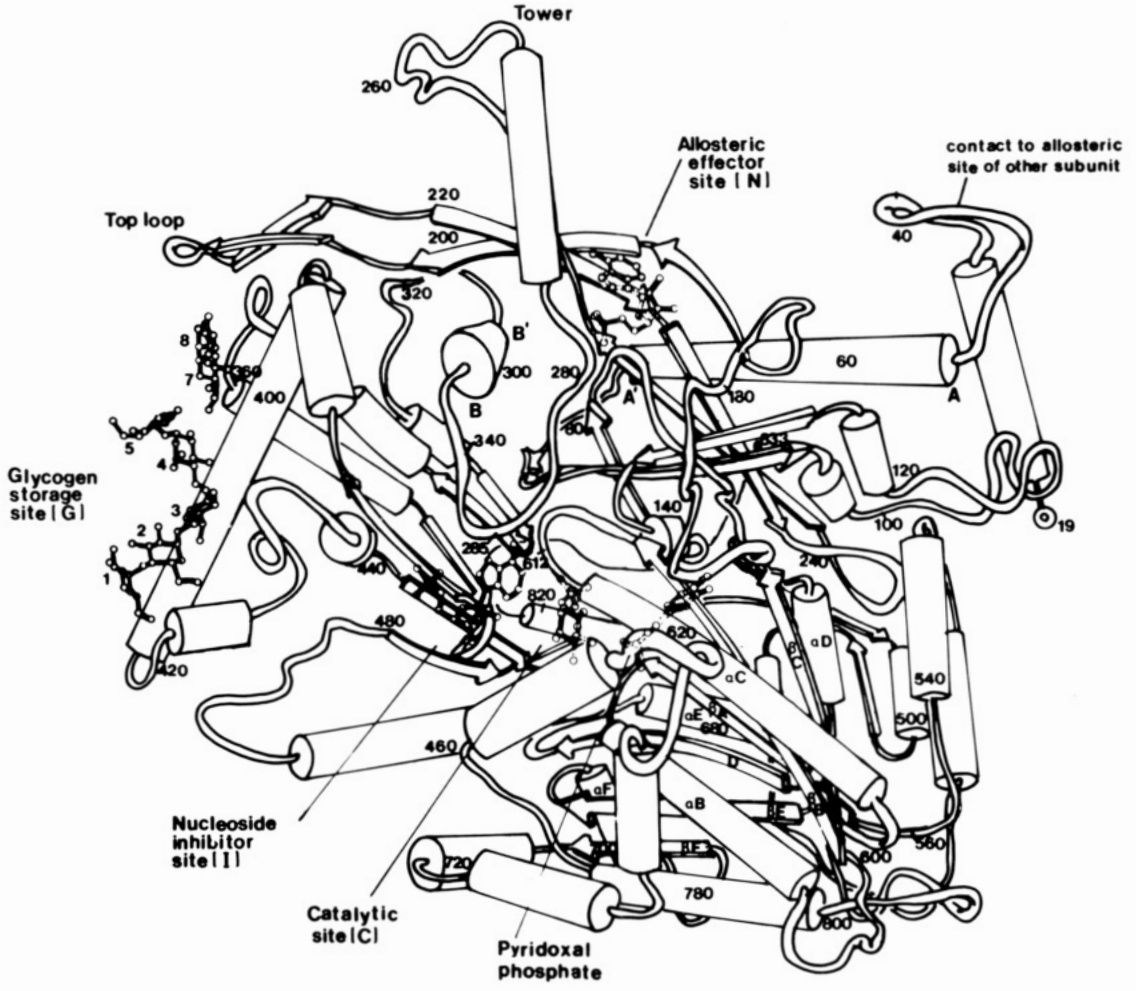

FIGURE 1: Schematic diagram of the phosphorylase *b* subunit viewed down the crystallographic *y* axis. α-Helices and β-strands are represented by cylinders and arrows, respectively. The first 18 residues from the N-terminus and the last 8 residues from the C terminus are not located in the native electron density map. Glucose 1-phosphate and pyridoxal phosphate (partially obscured by structural elements of the protein) are shown bound at catalytic site C, AMP at the allosteric effector site N, maltoheptaose at the glycogen storage site G, and AMP at the nucleoside inhibitor site I. The structural elements of the nucleotide binding domain are labeled (βA–αB, βB–αC, βC–αD, βD–αE, βE–αF, βF).

is close to the essential cofactor pyridoxal phosphate. The allosteric effector site (site N) is some 32 Å from site C. It utilizes residues solely from the N-terminal domain (residues 19–320) and is close to the subunit–subunit interface. The glycogen storage site (site G) is situated on the surface of the enzyme and is about 30 and 39 Å from the catalytic site and allosteric effector site, respectively. The amino acid sequence of phosphorylase, which is essential for interpretation of the X-ray results, has been determined by Titani et al. (1977).

The cofactor is buried in a location where residues from different structural domains come together. Solvent contact area calculations show that over 90% of its surface area is inaccessible to water. The cofactor is linked via a Schiff base to the ϵ-amino group of Lys-679. The aliphatic part of the lysyl side chain is extended as would be expected in order to accomodate the bulk cofactor. The Schiff base is almost planar and has the *trans configuration.* There is a hydrogen bond between the Schiff base nitrogen and the O3-hydroxyl group of the pyridoxal ring (Sansom et al., 1984).

The pyridoxal ring fits snugly into a hydrophobic pocket deep in the enzyme molecule and makes contacts with the structural elements of the "nucleotide binding domain" of phosphorylase including residues 567–569 (βA strand), 573 (βA–αB loop), 647–649 (βC–αD loop), 652 (αD), 671 and 674 (βD–αE loop), and 675–679 (αE) and to residues from the N-terminal domain "glycine" loop including residues

Table II: Summary of Possible[a] Interactions between Phosphorylase *b* and Pyridoxal Phosphate

cofactor atom	protein atom	side chain
	Hydrogen Bonds and Ionic Interactions	
O3	NZ	Lys-679
phosphorus	NZ	Lys-567
O11	N	Thr-675
	N	Gly-676
	ND2	Asn-677
phosphorus	NZ	Lys-567
O22	NZ	Lys-573
phosphorus O33	N	Gly-135
	van der Waals Interactions	
N1		Gly-134, Lys-567, Tyr-647
C2		Tyr-90, Tyr-647, Val-649
C2′		Tyr-647, Val-649
C3		Tyr-647, Val-649
O3′		Trp-490, Tyr-647, Val-649, Ala-652
C4		Lys-567
C5		Gly-134, Lys-567, Tyr-647
C5′		Gly-134, Gly-135, Lys-567, Thr-675, Gly-676
O5′		Lys-567, Thr-675, Gly-676

[a] These interactions appear plausible in terms of our current interpretation of the model, but they are tentative until the refinements of the native and complex structures are complete. Asn-284, in particular, is subject to some uncertainty (see text).

Table III: Summary of Possible[a] Interactions between Phosphorylase *b* and Heptulose 2-Phosphate

sugar atom	protein atom	side chain
Hydrogen Bonds and Ionic Interactions with Polar Groups		
O1	N	Leu-136 (bent)
O2	ND2	Asn-284[a]
	OH	Tyr-572
O3	OE1	Glu-671
	N	Ser-673
O4	ND2	Asn-483
	N	Gly-674
O5	ND1	His-376[c]
O6	ND1	His-376[c]
phosphorus O7	N	Gly-135 (bent)
	NZ	Lys-573
phosphorus O8	ND2	Asn-284[a]
phosphorus O9	O33	pyridoxal phosphate[b]
van der Waals Interactions with Nonpolar Groups		
C1		Leu-136, Asn-284, His-376
C2		His-376, Ala-672
C3		Ala-672, Gly-674
C4		His-376, Asn-483, Ala-672, Gly-674
C5		Gly-135, Leu-136, His-376
C6		Gly-135, Leu-136, His-376
C7		Leu-136, Asn-284,[a] His-376, Thr-377

[a] These interactions appear plausible in terms of our current interpretation of the model, but they are tentative until the refinements of the native and complex structures are complete. Asn-284, in particular, is subject to some uncertainty (see text). [b] The numbering system of the pyridoxal ring follows that conventionally used and is described in Sansom et al. (1983). [c] His-376 moves away from the sugar (~1.5 Å) in order to make this contact.

133–139 and Tyr-90. A summary of the contacts is given in Tables II and III. If, according to convention, we define the A face and the B face as those in which the numbering system appears in a clockwise and anticlockwise direction, respectively, then the major interaction involves the B face with the side chain of Tyr-647 (closest contact ≃ 3 Å and interplanar angle between the rings of 41°). The same face also interacts with the aliphatic side-chain atoms (CD and CE) of Lys-567. The A face of the pyridoxal ring is in van der Waals contact with Tyr-90, Gly-134, Gly-135, and Val-649. The ring nitrogen does not appear to be involved in any polar interactions. The nearest non-carbon atom is the carbonyl oxygen of residue 648, 4.3 Å away. Likewise, the O3′ hydroxyl does not make any other polar contacts apart from that to the NZ of Lys-679.

The 5′-phosphate group of the cofactor interacts via one of its oxygens (O11) with the NZ atom of Lys-567, with the side chain of Asn-677, and with the main-chain N atoms of Thr-675 and Gly-676. These last two residues lie at the start of the αE helix (residues 675–691) of the nucleotide binding domain, and since the amino-terminal end of this helix is buried, the stabilization of the phosphate by the helix dipole (Hol et al., 1978) is likely to be strong. Another phosphate oxygen (O22) interacts with the NZ atoms of Lys-567 and Lys-573. The third phosphate oxygen (O33) makes a distant contact with the main-chain N of Gly-135 and is the only phosphate oxygen accessible to water. Thus, the 5′-phosphate is firmly held by helix dipole interactions, by contacts with two cationic groups (Lys-567 and Lys-573), and by a hydrogen bond to Asn-677.

Heptenitol Binding. The heptenitol difference Fourier synthesis showed a single peak located at the catalytic site [maximum peak height 1.3 arbitrary units; estimated root mean square error in the difference synthesis (Blundell & Johnson 1976) 0.20 unit]. The single-crystal structure of heptenitol itself is not known. Observations with molecular models suggest that the trigonal carbon at C1 can be incorporated into the chair form of the glucopyranose ring without significant distortion. The standard glucose ring (Arnott & Scott, 1972) was modified accordingly with a trigonal carbon at C1 and the C1–C7 double bond adjusted to 1.34 Å. The resulting satisfactory fit to the observed difference electron density is shown in Figure 2A. A comparison of the coordinates with those obtained independently for the glucopyranose moieties of glucose (Sansom, 1983), glucose 1-phosphate (Johnson et al., 1980), and glucose cyclic 1,2-phosphate (Jenkins et al., 1981) shows no systematic differences.

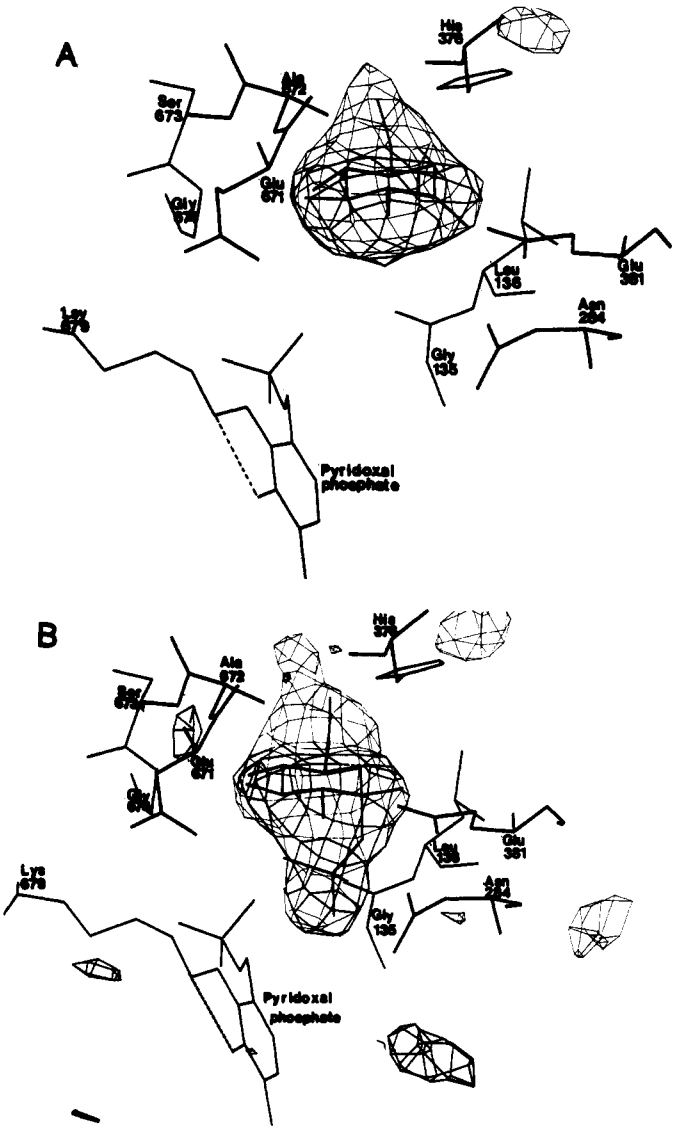

FIGURE 2: (A) Difference electron density for heptenitol bound at the catalytic site of phosphorylase *b* with the fit for heptenitol and surrounding protein atoms superimposed. Positive contours, 0.39 unit, only are shown. (B) Difference electron density for heptulose 2-phosphate bound at the catalytic site of phosphorylase *b* with the fit for heptulose 2-phosphate and surrounding protein atoms superimposed. Positive contours, 0.39 unit, only are shown.

There are two localized regions where small conformational changes occur. There are positive and negative features that indicate movement of His-376 (about 1.5 Å) in order to relieve overcrowding at the O6 hydroxyl group of heptenitol. A good hydrogen bond is then formed between ND_1 of His-376 and O6. Secondly, the C7 atom and, to some extent, C1 and O5 come close to the "glycine loop" in the region of Leu-136, and there are weak negative contours indicating movement away of the protein.

Apart from these movements, there are no indications of other changes in the structure, although a more precise analysis after crystallographic least-squares refinement may well identify other movements. Details of the interactions of heptenitol with the protein are discussed in the next section.

Heptulose 2-Phosphate–AMP–Maltoheptaose Complex. The difference Fourier synthesis contained three peaks that were interpreted as (i) heptulose 2-phosphate binding at site C (peak height 1.53 units), (ii) AMP binding weakly at site N (peak height 0.86 unit), (iii) oligosaccharide at site G (peak height 1.35 units). There were no other binding sites occupied. The root mean square error in the map was 0.22 unit.

Site C. It was immediately clear from the distribution of electron density at site C that conversion to a phosphorylated product had taken place. There was density for the glucopyranose moiety that corresponded with that observed for heptenitol, and additional higher density for the phosphate. Although unambiguous determination of chemical structure is not possible from electron density maps at 3-Å resolution, the shape and peak heights are consistent with the structure expected for heptulose 2-phosphate (Figure 2B). Observations with models showed that if the torsion angle about C1–O1 is similar to that for glucose 1-phosphate (i.e., O5–C1–O1–P = 117°, close to the preferred conformation for α(1–4) glycosidic links), then there is a bad contact between the α-linked phosphate oxygens and the β-linked C7 methyl group. This bad contact can be relieved by a change in the torsion angle. The best fit to the density was achieved with the glucopyranose in the standard chair conformation and the torsion angle for the phosphate ester O5–C1–O1–P = −136°. With this conformation, there is an internal hydrogen bond between one of the phosphate oxygens (O8) and O2 hydroxyl of the sugar, so that the structure roughly resembles that of glucose cyclic 1,2-phosphate where the corresponding torsion angle is −144° (Jenkins et al., 1981; Sansom et al., 1984). The difference electron density also indicated the position of the C7 methyl group (Figure 2B).

Indications of the movement of His-376 and of Leu-136 are also observed in the heptulose 2-phosphate difference map. As a result of the tetrahedral geometry at C1 in the phosphorylated molecule, there is no longer overcrowding between Leu-136 and C7 group. However, the region of Leu-136 is close to His-376, and the movements of these residues may be correlated. In addition, the difference map indicates some disturbances around the pyridoxal ring and the side chains of Arg-574, Asn-677, and Asp-283. The latter residue appears to shift so that it is closer to His-570. Detailed analysis of these movements must await refinement.

The catalytic site is formed where loops from the different structural domains of phosphorylase come together. The relevant residues include (N-terminal domain) residues 135–136 (glycine loop) and 284, (glycogen storage domain) residues 376–377, 454, and 483 (C-terminal domain) residues 572–573 and 671–675 (the βA–αB and βD–αE loops of the nucleotide binding domain), and Lys-679 and the pyridoxal phosphate cofactor. A summary of van der Waals interactions and possible hydrogen bonds for heptulose 2-phosphate is given in Tables II and III. The sugar is held in place by hydrogen bonds to each of its polar groups and by satisfactory van der Waals interactions with its other atoms. The phosphate is stabilized by the fractional positive charge arising from the dipole of helix residues 135–149, an ionic interaction with Lys-573, a hydrogen bond to Asn-284, and the contact between O9 of the heptulose 2-phosphate and the pyridoxal phosphate oxygen O33 (Figure 3). The latter contact appears most

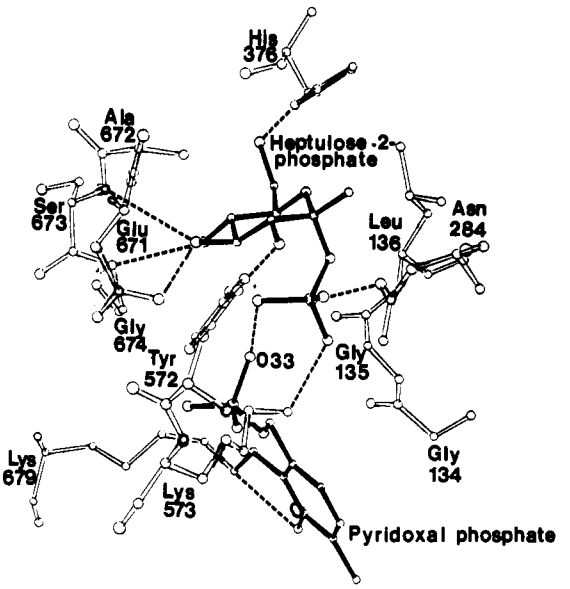

FIGURE 3: Interactions of heptulose 2-phosphate with glycogen phosphorylase *b*. Possible hydrogen bonds are shown dotted.

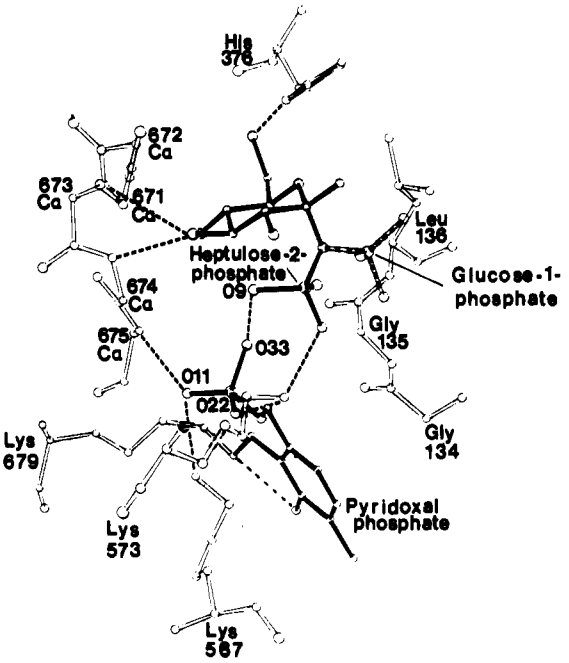

FIGURE 4: Comparison of positions and environments of phosphate groups of pyridoxal phosphate, heptulose 2-phosphate, and glucose 1-phosphate (P–O bond shown stippled). Asn-284, Tyr-572, and Asn-677 are not shown for clarity.

significant. The separation of phosphate oxygen to phosphate oxygen is 2.7 Å, and there is presumably a hydrogen bond between them.

The distance between the phosphorus atoms of heptulose 2-phosphate and pyridoxal phosphate is 4.5 Å. The heptulose 2-phosphate phosphorus position is similar to that of glucose cyclic 1,2-phosphate but not identical with it (difference in position of phosphorus atoms 1.2 Å). Comparison of the positions of glucose 1-phosphate and heptulose 2-phosphate shows that the glucopyranose moieties bind in essentially the same way but that their phosphorus positions differ by 2.3 Å (Figure 4). In the glucose 1-phosphate complex, the distance between the phosphorus atoms of the substrate and the cofactor is 6.5 Å, and the closest approach of their phosphate oxygens is 5.4 Å. A recent kinetic study by Chang et al. (1983) with pyridoxal-reconstituted apophosphorylase activated with

phosphite led these authors to the conclusion that the bound phosphite in pyridoxal phosphorylase and, possibly, the 5′-phosphoryl group of pyridoxal phosphate in native phosphorylase do not effect the glucose 1-phosphate binding. The phosphate of glucose 1-phosphate is stabilized by a helix dipole interaction involving the main-chain N of Leu-136. The phosphoryl group makes rather too close contacts with the side chain of Asn-284, and in the glucose 1-phosphate difference map there are indications of movement of this residue.

Comparison of the contacts between phosphorylase *b* and heptenitol, glucose 1-phosphate, and heptulose 2-phosphate with those between phosphorylase *a* and glucose and glucose cyclic 1,2-phosphate (Sprag et al., 1982; Withers et al., 1982a) shows that there are similarities in the portions of protein involved and some interactions appear identical. For example, His-376 interacts with the glucopyranose O6 hydroxy and O5 ring oxygen atoms in both cases. But in the phosphorylase *a* complexes, His-376 moves toward the sugar while in the phosphorylase *b* complexes it moves away from the sugar. Since His-376 is linked via a buried ionic interaction to Asp-338 and by van der Waals interactions to Leu-136, these movements may be significant for catalysis and allostery. The phosphorylase *a* crystals are grown in the presence of the inhibitor glucose and are generally assumed to be in the T state. Significant conformational changes take place in these crystals on binding substrates. The phosphorylase *b* crystals are grown under conditions in which the enzyme is partially active (as described in the introduction), and the conformational changes on binding substrate are relatively minor. The differences in substrate contacts between complexes with phosphorylase *a* and with phosphorylase *b* may be real or may be due to differences in interpretation of the structure of the native enzyme. However, the position of the 5′-phosphate of the cofactor is quite unambiguous in both structures. In phosphorylase *a*, the separation (phosphorus to phosphorus) of the glucose cyclic 1,2-phosphate is 6.8 Å (Withers et al., 1982a) whereas in phosphorylase *b* the separation for glucose cyclic 1,2-phosphate is 5.3 Å (Jenkins et al., 1981) and for heptulose 2-phosphate is 4.5 Å. These distances represent genuine differences in the way in which the substrates and inhibitors interact with the two forms of the enzyme.

Site N. The difference electron density indicates that AMP at 2.5 mM binds weakly to site N. The peak height was 68% of that observed in a similar binding study in which the AMP concentration was 100 mM (N. Oikonomakos, unpublished results). In fact, the peak could best be distinguished in the map based on $F_{H2P} - F_{Hept}$ as coefficients, presumably because the native structure factor amplitudes are derived from crystals grown in the presence of 2 mM IMP and contain IMP bound weakly at site N. Also, the data from heptulose 2-phosphate–AMP–maltoheptaose complex and the heptenitol complex were collected and processed by the same method so that any possible systematic errors cancel out. The adenine and ribose portions of AMP occupy similar positions to those previously reported (Stura et al., 1983). There is also an indication of movement of Tyr-75 toward the base. The peak for the phosphate is broad and has its maximum approximately midway between the two phosphate sites identified at this site (Lorek et al., 1984). The previously observed phosphate positions for AMP and for inorganic phosphate were both in the density with the peak minimum between them. It is of interest that a similar shift in the phosphate position of AMP is seen in binding studies both with 100 mM AMP–100 mM glucose 1-phosphate and with 100 mM AMP–100 mM inorganic phosphate (N. Oikonomakos, unpublished results).

Site G. Binding studies with a variety of oligosaccharides have identified a "glycogen storage" site, site G, on the surface of phosphorylase to which linear oligosaccharides bind preferentially (Johnson et al., 1983). No binding of oligosaccharide at the catalytic site has been observed. At site G the oligosaccharides adopt a conformation close to the preferred conformation for $\alpha(1-4)$-linked glucopyranoses [e.g., Rees & Smith (1975)]. The amylose-like helix curves toward the long polypeptide helix that extends from residue 397 to 417. In the presence of other ligands (e.g., IMP at site N or glucose cyclic 1,2-phosphate at site C), maltoheptaose binds with five sugars localized in subsites 1–5 with the reducing end in subsite 5. In the absence of other ligands, two further sites, subsites 7 and 8, are filled. There is a break in the electron density between subsites 5 and 7.

In the present studies, where both site C and site N are occupied, maltoheptaose was found bound to sites 1–5, and there was extra density indicating a further subsite (site "0"). The sugar in site 0 does not appear to make contact to the protein. There was no oligosaccharide bound in sites 7 and 8. A detailed discussion of the oligosaccharide conformation and protein contacts will be published elsewhere. We note, however, that two interpretations of the electron density appear possible, one with the reducing end of the bound hexasaccharide in site 5 and other with the reducing end in site 0. We hope to resolve this problem with studies employing an asymmetrically labeled oligosaccharide.

Heptenitol Reaction in Crystals. Incubation of crystals of phosphorylase *b* in a solution containing 100 mM heptenitol, 50 mM phosphate, 2.5 mM AMP, and 50 mM maltoheptaose gave rise to no detectable product after 1 h. Product with an R_f value corresponding to that of heptulose 2-phosphate was detected after 24 and 50 h. No heptulose 2-phosphate was detected even after 50 h in control experiments in which either the phosphorylase crystals or the oligosaccharide had been omitted. In all these experiments, a small amount of heptitol, the hydrolysis product of heptenitol, was apparent.

In an experiment, designed to test whether enzyme molecules had dissolved from the crystal into the soak solution and could themselves promote catalysis, heptulose 2-phosphate was detected after a second 50-h incubation with the soak solution alone. Again, no product was formed either if the phosphorylase crystal was omitted (in the first soak) or if oligosaccharide was omitted throughout. A small amount of glucose 1-phosphate was detected in the third control experiment in which heptenitol was omitted. The results from these experiments suggest that there is sufficient dissolution of the suface layer of enzyme molecules into the surrounding soak solution over long periods of time (50 h) and that these enzyme molecules can promote catalysis. The R_f values for glucose 1-phosphate and heptulose 2-phosphate are similar, so it is not known whether glucose 1-phosphate is also formed in the presence of heptenitol. However, the breakdown of oligosaccharide appeared to be minimal in the heptenitol experiment. This is discussed in a forthcoming paper (H. W. Klein, D. Palm, M. J. Im, and G. Blumenauer, unpublished results).

The results of these experiments show that oligosaccharide is essential for the conversion of heptenitol to heptulose 2-phosphate. Previous kinetic and covalent modification studies (Kasvinsky et al., 1978; Sotiroudis et al., 1978; Shimomura & Fukui, 1980; Philip et al., 1982) have demonstrated that the first step in the association of rabbit muscle phosphorylase with glycogen involves the occupation of the high-affinity glycogen storage site ($K_D \simeq 1$ mM). Binding of oligosaccharide at this site results in enhanced catalytic activity:

over a 10-fold increase in activity is observed if phosphorylase *a* is preincubated with glycogen. The oligosaccharide bound at the glycogen storage site does not participate directly in catalysis, since terminal 4-*O*-methylmaltoheptaose covalently bound at the storage site does not affect activity (Philip et al., 1982). Rabbit muscle phosphorylase, in contrast to the potato and *Escherichia coli* maltodextrin phosphorylases (which both lack a glycogen storage site), has a much higher affinity for branched oligosaccharide substrates such as glycogen than for linear oligosaccharides. The K_m values for these subtrates differ by approximately 400-fold (Hu & Gold, 1975). However, the storage site does not appear to play a role in determining this specificity since K_m values for glycogen and maltoheptaose still differ by 2 orders of magnitude in a modified phosphorylase in which oligosaccharide is covalently linked to the storage site (Philip et al., 1982). The present crystallographic results show that oligosaccharide is bound at the glycogen storage site under conditions in which the heptenitol to heptulose 2-phosphate conversion takes place and that the presence of oligosaccharide is obligatory for this reaction. The mechanism of activation by oligosaccharide remains elusive. No direct interactions between the storage site and the catalytic site are observed, and no obvious conformational changes take place.

Discussion

The results described in this paper show that the incubation of a phosphorylase *b* crystal with heptenitol and inorganic phosphate, together with AMP and oligosaccharide as activators, leads to the binding at the catalytic site of a phosphorylated product whose electron density is consistent with heptulose 2-phosphate. Analysis of the surrounding soak solution by thin-layer chromatography showed that heptulose 2-phosphate was either not formed or not released into the solution during the first hour of reaction. Product was detected after 24 h. After 50-h incubation (the time used in the X-ray diffraction experiment), there was sufficient enzyme in the surrounding solution to bring about some catalysis. These enzyme molecules probably came from dissolution of the surface layer of the crystal. Thus at the present stage, because of the relatively long soak time, we cannot definitively state that catalysis took place in the crystal during the X-ray experiment rather than in the surrounding mother liquor. Further studies on the time course of the reaction in the crystal are required in order to answer this question. Nevertheless, a number of lines of evidence favor the idea of catalysis in the crystal. The crystals of phosphorylase *b* are known to be active (Kasvinsky & Madsen, 1976), even though the catalytic events are likely to be limited by the diffusion time of substrate into the crystal (Makinen & Fink, 1977). Experiments indicate that binding sites in the crystal (dimensions approximately 1 mm × 0.3 mm × 0.3 mm) are saturated after a soak time of 10 min (L. N. Johnson, unpublished observations). In previous crystallographic studies, we have observed catalysis by phosphorylase crystals with glucose 1-phosphate and oligosaccharide as substrates (Sansom et al., 1984; J. Hajdu, unpublished work).

However, even the long soak times and high concentrations, the reverse reaction (oligosaccharide and phosphate to glucose 1-phosphate) has not been observed in the crystal. This is of relevance to the present work where these substrates (oligosaccharide and phosphate) were present in the soak solution. The equilibrium constant is dependent on pH and is determined by the ratio [inorganic phosphate]/[glucose 1-phosphate]. At pH 6.8, the ratio is 3.6 (Graves & Wang, 1972). Hence, the reaction is less favorable in the direction of glucose 1-phosphate formation. Under the conditions of the crystal experiment, the concentration of glucose 1-phosphate if formed would be less than its dissociation constant. No glucose 1-phosphate binding was observed in the crystal. In a control experiment with oligosaccharide and phosphate, the thin-layer chromatography showed that after 50 h the mother liquor produced a very small amount of glucose 1-phosphate. The failure of the crystalline enzyme to produce detectable glucose 1-phosphate may also be due to the fact that oligosaccharide cannot bind readily at the catalytic site in the crystal (Johnson et al., 1980).

The present X-ray results clearly show that there are marked differences in the phosphate positions of enzyme-bound glucose 1-phosphate (K_m = 37 mM in the presence of IMP; K_m = 3 mM in the presence of AMP) and of enzyme-bound heptulose 2-phosphate (K_i = 14 μM) (Figure 4). Since the glycopyranose moieties bind in essentially the same position, the differences in affinity must be attributed to their different phosphate positions (which are related by a rotation about the glycosidic C1–O1 bond). Both phosphates are stabilized by the helix dipole from the helical residues 135–149. However, the phosphate of heptulose 2-phosphate makes additional favorable interactions with the side chains of Lys-573 and Asn-284 and with the 5′-phosphate of pyridoxal phosphate. The phosphate of glucose 1-phosphate makes rather too close contacts with Asn-284. (However, the region 282–284 has proved difficult to build, with rather large amounts of extra electron density in the native map. In phosphorylase *a*, movements in this region are seen on binding substrates). The additional interactions made by the phosphate of heptulose 2-phosphate appear sufficient to account for the apparently tighter binding of this material. Transition-state theory suggests that a substrate analogue that resembles the transition state of the catalyzed reaction should bind several orders of magnitude tighter than the substrate itself (Pauling, 1946; Wolfenden, 1969). The tight binding of heptulose 2-phosphate, a product formed by phosphorylase, suggests it may be a good candidate for a transition-state analogue. The phosphate position occupied by heptulose 2-phosphate could therefore be the "catalytic" phosphate position. We call this position the "down" position (with reference to the crystallographic *z* axis). The structural results suggest that this position can only be reached in the presence of a steric constraint such as that imposed by the C7 β-methyl group in heptulose 2-phosphate or by the cyclic structure of glucose cyclic 1,2-phosphate.

In considering the catalytic reaction with the natural substrates glucose 1-phosphate and glycogen, we suggest that the presence of glycogen encourages the phosphate to its down catalytic position. Substrate interconversion would then only take place within the ternary enzyme–substrate complex. Indeed, with the phosphate in the down position there is greater scope for approach of the oligosaccharide while still allowing the reaction to proceed with retention of configuration. Such considerations also help to explain why heptulose 2-phosphate is a dead-end product: the presence of the β-methyl group provides a strong steric constraint against the approach of oligosaccharide. We must, however, still be cautious about the role of oligosaccharide in catalysis since we have no data on oligosaccharide binding at the catalytic site in the crystal. We note from model-building studies that there is overcrowding at the second sugar site with the loop of chain in the region of Gly-135 and that either there must be distortion of the oligosaccharide from its preferred conformation or there must be a shift in the protein conformation before oligosaccharide can bind. Our present discussions of mechanism

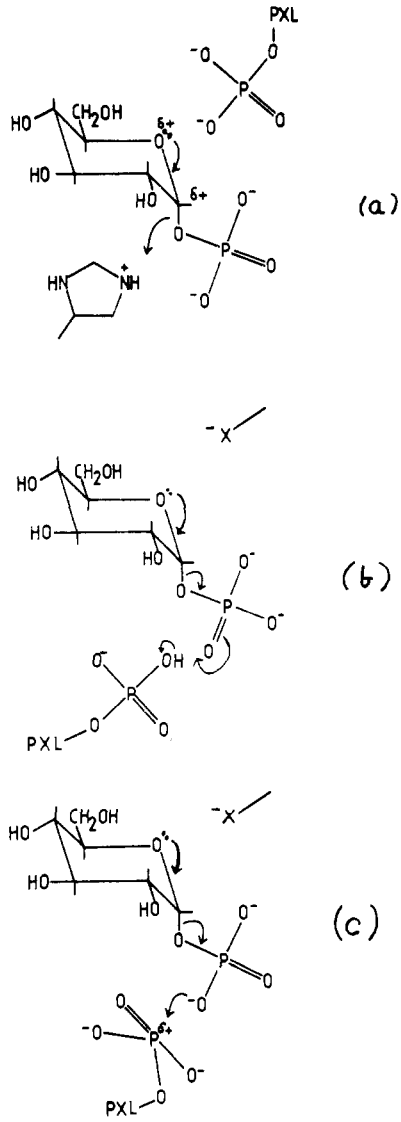

FIGURE 5: Proposals for possible role of 5′-phosphate of pyridoxal phosphate in phosphorylase catalysis: (a) 5′-phosphate as a nucleophile or electrostatic group (Johnson et al., 1980; b) 5′-phosphate as a general acid–base catalyst (Klein et al., 1982); (c) phosphorus of 5′-phosphate as an electrophile (Withers et al., 1981b). PXL is pyridoxal.

are therefore limited to what we can learn from the results on the heptenitol reaction.

Mechanisms that have been proposed for the role of the 5′-phosphate of pyridoxal phosphate in catalysis are summarized in Figure 5. We note that the reaction proceeds, through cleavage of the C–O bond of glucose 1-phosphate, with retention of configuration and that the kinetics demonstrate a random-order bi-bi mechanism in which the rate-limiting step involves the interconversion of the ternary enzyme–substrate complexes (Graves & Wang, 1972). There is some evidence for involvement of a glucosyl cation or glucosyl–enzyme intermediate (Tu et al., 1971; Firsov et al., 1974; Kokesh & Kakuda, 1977). Rate (V_{max}) vs. pH profiles show a bell-shaped curve with apparent pK_a values at 5.2 and 7.2 (Withers et al., 1982c). Kasvinsky & Meyer (1977) noted a pK_a of 6.56 associated with the ionization of substrate. In the work of Withers et al. (1982c), a pK_a of approximately 7.2 was observed for the dependence of K_m on pH.

Pyridoxal Phosphate as a Nucleophile or an Electrostatic Stabilizing Group (Figure 5a). In 1980, we noted (1) the change in the state of ionization of the 5′-phosphate from a monoanion to a dianion following the conversion of the regulatory phosphorylases from the inactive to the active state (Feldmann & Hull, 1977), (2) the likely requirement for an electrostatic interaction to stabilize the transition-state carbonium ion intermediate, and (3) the need to accommodate oligosaccharide at the active site (Johnson et al., 1980). In order to reconcile the available evidence, we proposed that the mode of binding of the glucose 1-phosphate as seen in the X-ray structure represented a nonproductive mode. We showed by molecular model-building studies than an alternative binding mode was possible that would allow oligosaccharide to bind in its preferred conformation to the active site channel. It was proposed that the 5′-phosphate dianion could act to stabilize the carbonium ion intermediate and that His-376 could act as a general acid (Figure 5a). The close proximity of the carbonium ion to the pyridoxal 5′-phosphate could result in a perturbation of its ^{31}P NMR spectra consistent with the studies that have been reviewed by Helmreich & Klein (1980). Takagi et al. (1981) have since reconstituted apophosphorylase with pyridoxal(5′)phospho(1)-β-D-glucose and shown that this complex has no enzyme activity. β-D-Glucopyranose 1-phosphate does not appear to bind to the pyridoxal enzyme (Withers et al., 1982a). These results rule our participation of the 5′-phosphate of pyridoxal phosphate as a nucleophile that acts to form a covalent intermediate, but they do not exclude electrostatic stabilization of the carbonium ion by the phosphate dianion of the cofactor. Although this mechanism has the advantage of simplicity, there is no direct evidence to support it.

We now have difference electron density maps for five substrates and substrate analogues bound at the catalytic site of phosphorylase *b* (glucose 1-phosphate, glucose, heptenitol, glucose cyclic 1,2-phosphate, and heptulose 2-phosphate). The last two compounds are potent inhibitors (K_i = 500 μM and 26 μM, respectively; Klein et al., 1984b) and may be related to the transition-state structure for the reaction. All of these compounds bind with their glucopyranose moieties in essentially the same position, indicating that the enzyme is specific for this part of the substrate. The observations for heptulose 2-phosphate seem to us to be the most relevant for catalysis, because this compound is formed in a catalytic reaction of the enzyme. The orientation of this compound is not compatible with the nucleophilic or electrostatic role of the cofactor phosphate envisaged by Johnson et al. (1980).

Pyridoxal Phosphate as an Acid–Base (Figure 5b). On the basis of ^{31}P NMR data and the reaction of phosphorylase with glycosylic substrates such as heptenitol and glucal (Helmreich & Klein, 1980; Klein et al., 1982; 1984a,b), Helmreich and his colleagues have proposed a mechanism in which the 5′-phosphate group of pyridoxal phosphate becomes protonated when substrate binds and that this group then acts as a general acid to catalyze the cleavage of glucose 1-phosphate (Figure 5b). This mechnism can explain why the enzyme catalyzes phosphorylysis rather than hydrolysis, as discussed by Jenkins et al. (1981).

The NMR observations reported in the preceding paper (Klein et al., 1984) indicate the dianionic 5′-phosphate group of the natural cofactor becomes partially protonated on binding heptulose 2-phosphate to potato phosphorylase whereas the monoprotonated 5′-phosphonate group of the partially active deoxypyridoxal(methylenephosphonate) phosphorylase *b* derivative was shown to share a proton with the phosphate moiety of heptulose 2-phosphate. In the crystal studies on phosphorylase *b* with the natural cofactor, the separation of the heptulose 2-phosphate and cofactor phosphate oxygen atoms is 2.7 ± 0.3 Å. There are no charged groups in the immediate

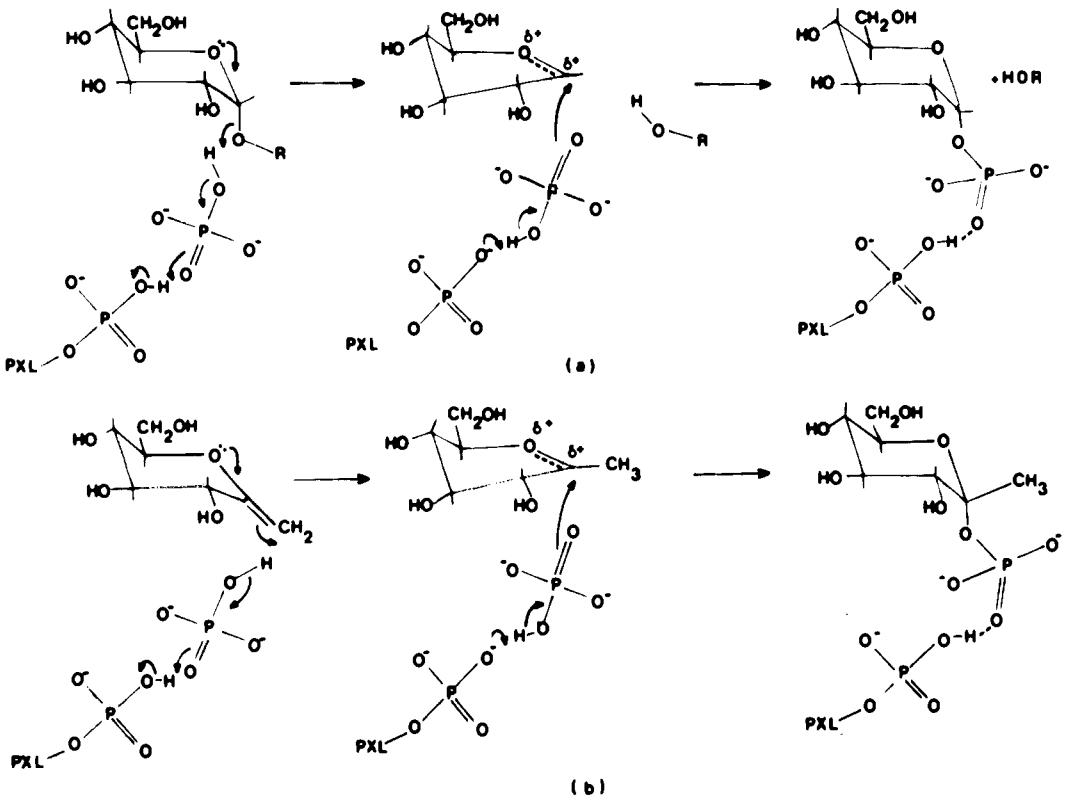

FIGURE 6: Proposed schemes for the phosphorylation of (a) glycogen and (b) heptenitol that involve the 5′-phosphate of pyridoxal phosphate as a general acid–base catalyst.

vicinity of these electronegative atoms, and we must therefore assume there to be a hydrogen bond between them. On the basis of the X-ray evidence, we cannot tell with which phosphate the proton is associated.

A neutron diffraction study, like that carried out on trypsin by Kossiakoff & Spencer (1980), would be required to solve this problem. We note that the pK_a of heptulose 2-phosphate is 6.7 while the pK_a of the cofactor phosphate is sensitive to the state of activation of the enzyme.

As noted previously (Johnson et al., 1980), the 5′-phosphate of the pyridoxal phosphate is too far from the glycosidic oxygen to act directly as a general-acid catalyst at this locus. However, the close proximity of the two phosphates observed in the heptulose 2-phosphate complex is in accord with mechanism whereby the cofactor facilitates loss of inorganic phosphate from glucose 1-phosphate, as shown in Figure 5b.

In the reverse reaction it is envisaged that the cofactor phosphate promotes attack of inorganic phosphate on the glycoside (Figure 6a). The corresponding reaction whereby the constellation of groups observed in the crystal structure might result in phosphorylation of heptenitol is shown in Figure 6b. In the first step, the monoanion form of the cofactor promotes protonation of the carbon–carbon double bond by inorganic phosphate leading to a carbonium–oxonium ion intermediate. Subsequent nucleophilic attack by the inorganic phosphate results in the formation of heptulose 2-phosphate. The geometry of the active site ensures that the phosphate ester bond is in the α-configuration.

It is evident that such proposals form only the most simplified scheme. Even so, there are at least three uncertainties. First, there is no direct evidence that the proton comes from inorganic phosphate. It could come from the solvent or from a group on the enzyme. However, there is no suitable proton-donating group in the vicinity. In support of our proposals, we note that phosphate is obligatory for the reaction and that such a bifunctional role for phosphate has precedent in physical organic chemistry. The second uncertainty concerns the phosphate binding site itself. A shift in position (of approximately 1 Å) is required between the first stage of the reaction where the phosphate is noncovalently bound and the second stage where the phosphate is covalently attached to the heptulose 2-phosphate molecule. Our direct observations relate only to the final stage of the scheme. Clearly, it will be important to establish the phosphate attacking position, and this might be possible by low-temperature X-ray crystallographic studies. Third, the mechanism appears to require a group X^- (Figure 5b) to stabilize the carbonium–oxonium ion intermediate. In the present interpretation of the crystal structure, there are no obvious candidates. Glu-671 and Tyr-572 are in the vicinity but are in the wrong orientation and too distant with respect to the C1 atom. Glu-381 is in the right orientation (Figure 2b) but the carboxyl oxygens are more than 5 Å from C1. However, an attractive feature of the acid–base mechanism shown in Figures 5b and 6 is that the bifunctional role of the inorganic phosphate molecule allows it to act as its own nucleophile. Therefore, it may be that groups from the protein for this role are not of vital importance, although they are still likely to contribute some stabilization.

Pyridoxal Phosphate as an Electrophile (Figure 5c). Madsen and Fukui and their colleagues have together and independently provided evidence for the close proximity of the substrate's phosphate and the cofactor's 5′-phosphate groups (Shimomura & Fukui, 1980; Withers et al., 1981a,b, 1982a,b; Takagi et al., 1982; Fukui et al., 1984; Madsen & Withers, 1984). These observations have led them to propose that in the presence of substrate the dianionic phosphate group is constrained so as to allow the phosphorus atom to act as an electrophile (Figure 5c). The phosphorus atom withdraws electrons from the substrate phosphate and destabilizes the ester bond.

Part of the evidence for this mechanism came from X-ray

diffraction studies on phosphorylase *a* crystals complexed with glucose cyclic 1,2-phosphate in which the distance between the inhibitor phosphorus and the cofactor phosphorus was 6.8 Å (Withers et al., 1982a). In the present study, we observe the distance between the phosphorus of bound heptulose 2-phosphate and the cofactor phosphorus atom to be 4.5 Å. The closest approach of the heptulose 2-phosphate oxygen to the phosphorus of the cofactor is 3.9 Å. However, the electrophilic mechanism (Figure 5c) would presumably demand an even closer approach than this, and we may expect that the separation of substrate phosphate oxygen and the cofactor phosphorus would have to be only 2–3 Å for effective electrophilic catalysis.

It has been proposed (Withers et al., 1981a,b, 1982a) that additional cationic groups might move into the catalytic site during catalysis and help to stabilize the putative pentacoordinated state of the 5′-phosphorus atom. The present work on phosphorylase *b* shows that the 5′-phosphate is already buried in the native enzyme with only one phosphate oxygen (O33) accessible to water (or to other groups). On binding heptulose 2-phosphate, the 5′-phosphate of the cofactor becomes totally inaccessible. It seems therefore unlikely that there is room for any additional contributions to the phosphate stabilization in this particular complex. No movement of the 5′-phosphate or of any groups in its vicinity is observed in our difference Fourier syntheses, although at 3-Å resolution a change in geometry from tetrahedral to pentacoordinate at the phosphorus would be very difficult to detect.

One criticism of the "phosphorus as electrophile" hypothesis has been that if the incoming phosphate oxygen approach was "in line" with respect to the 5′-phosphate ester linkage, then the enzyme could function as a kinase, cleaving the 5′-phosphate ester bond and transferring the 5′-phosphate to glucose 1-phosphate. We note, however, that in the heptulose 2-phosphate complex (Figure 3) the approach of the substrate phosphate oxygen is definitely not in line.

The electrophilic mechanism requires a proton donor and a nucleophilic group (X^-) to stabilize the carbonium ion intermediate. As noted above, in our present crystal structure although there are some possible candidates for these roles, none of these amino acid side chains are close enough or in the right orientation. We therefore consider that our present X-ray evidence neither rules out the electrophilic mechanism nor provides evidence to support it.

In summary, our results demonstrate the close proximity of the phosphate of the product heptulose 2-phosphate to the 5′-phosphate of the pyridoxal phosphate, in an orientation that is consistent with a proton-transfer role for the 5′-phosphate of pyridoxal phosphate [see preceding paper, Klein et al. (1984b)]. The results do not rule out other possible mechanisms, nor are we able, as yet, to elucidate the binding mode of the second substrate glycogen, nor can we disregard the fact that more substantial changes in conformation may take place during activation and catalysis and that these changes may bring other groups into the active site region.

Acknowledgments

We are grateful to Professor E. J. M. Helmreich and his colleagues for many useful discussions and for making data available to us before publication. We acknowledge with thanks the gift of maltoheptaose from Boehringer Corp. We are grateful to Drs. G. Lowe and S. Salome for help with the thin-layer chromatography. Phosphorylase was prepared in the Enzyme Preparation Laboratory of the Oxford Enzyme Group. We acknowledge with thanks the help of Dr. J. Helliwell and the staff and technical support team for the use of the Synchrotron Radiation Source at the Science and Engineering Research Council's Laboratory, Daresbury. We are most grateful to Professor J. R. Knowles for his valuable comments on the manuscript and to Sir David Phillips for his encouragement and support of this work.

Registry No. AMP, 61-19-8; heptulose 2-phosphate, 92642-58-5; heptenitol, 74310-30-8; phosphate, 14265-44-2; maltoheptaose, 34620-78-5; pyridoxal 5′-phosphate, 54-47-7; glycogen phosphorylase *b*, 9012-69-5.

References

Arnott, S., & Scott, W. E. (1972) *J. Chem. Soc., Perkin Trans. 2*, 324–335.

Bernstein, F. C., Koetzle, T. F., Williams, G. J. B., Meyer, E. F., Brice, M. D., Rodgers, J. R., Kennard, O., Shimanouchi, T., & Tasmuni, M. (1977) *J. Mol. Biol. 112*, 535–542.

Black, W. J., & Wang, J. H. (1968) *J. Biol. Chem. 243*, 5892–5898.

Blundell, T. L., & Johnson, L. N. (1976) *Protein Crystallography*, Academic Press, London.

Chang, Y. C., McCalmont, T., & Graves, D. J. (1983) *Biochemistry 22*, 4987–4993.

Feldmann, K., & Hull, W. E. (1977) *Proc. Natl. Acad. Sci. U.S.A. 74*, 856–860.

Feldmann, K., Horl, M., Klein, H. W., & Helmreich, E. J. M. (1978) *Proc. FEBS Meet. 42*, 205–218.

Firsov, L. M., Bogacheva, T. I., & Breslev, S. E. (1974) *Eur. J. Biochem. 42*, 605–609.

Fischer, E. H., & Krebs, E. C. (1962) *Methods Enzymol. 5*, 369–373.

Fukui, T., Tagaya, M., Takagi, M., & Shimomura, S. (1983) in *Chemical and Biological Aspects of Vitamin B_6 Catalysis* (Evangelopoulos, A. E., Ed.) pp 161–170, Liss, New York.

Graves, D. J., & Wang, J. H. (1972) *Enzymes, 3rd Ed. 7*, 435–482.

Hehre, E. J., Brewer, C. F., Uchiyama, T., Schlesselman, P., & Lehmann, J. (1980) *Biochemistry 19*, 3557–3564.

Helliwell, J. R., Greenhough, T. J., Carr, P. D., Rule, S. A., Moore, P. R., Thompson, A. W., & Worgan, J. S. (1982) *J. Phys. E. 15*, 1363–1372.

Helmreich, E. J. M., & Klein, H. W. (1980) *Angew. Chem., Int. Ed. Engl. 19*, 441–455.

Hendrickson, W. A., & Konnert, J. H. (1980) in *Biomolecular Structure, Function, Conformation and Evolution* (Srinivasan, R., Ed.) Vol. 1, pp 43–57, Pergamon Press, Oxford.

Hol, W. G. J., Van Duijnen, P. T., & Berendsen, H. J. C. (1978) *Nature (London) 273*, 443–446.

Hu, H. Y., & Gold, A. M. (1975) *Biochemistry 14*, 2224–2230.

Jenkins, J. A., Johnson, L. N., Stuart, D. I., Stura, E. A., Wilson, K. S., & Zanotti, G. (1981) *Philos. Trans. R. Soc. London, Ser. B 293*, 23–41.

Johnson, L. N., Madsen, N. B., Mosley, J., & Wilson, K. S. (1974) *J. Mol. Biol. 90*, 703–717.

Johnson, L. N., Jenkins, J. A., Wilson, K. S., Stura, E. A., & Zanotti, G. (1980) *J. Mol. Biol. 140*, 565–580.

Johnson, L. N., Stura, E. A., Sansom, M. S. P., & Babu, Y. S. (1983) *Biochem. Soc. Trans. 11*, 142–144.

Jones, T. A. (1978) *J. Appl. Crystallogr. 11*, 272–288.

Jones, T. A. (1982) in *Computational Crystallography* (Sayre, D., Ed.) pp 303–317, Clarendon Press, Oxford.

Kavinsky, P. J., & Madsen, N. B. (1976) *J. Biol. Chem. 251*, 6852–6859.

Kasvinsky, P. J., & Meyer, W. L. (1977) *Arch. Biochem. Biophys. 181*, 616–631.

Kasvinsky, P. J., Madsen, N. B., Fletterick, R. J., & Sygusch, J. (1978a) *J. Biol. Chem. 253*, 1290–1296.

Kasvinsky, P. J., Madsen, N. B., Sygusch, J., & Fletterick, R. J. (1978b) *J. Biol. Chem. 253*, 3343–3351.

Klein, H. W., Palm, D., & Helmreich, E. J. M. (1982) *Biochemistry 21*, 6675–6684.

Klein, H. W., Im, M. J., & Helmreich, E. J. M. (1984a) in *Chemical and Biological Aspects of Vitamin B_6 Catalysis* (Evangelopoulos, A. E., Ed.) pp 147–160, Liss, New York.

Klein, H. W., Im, M. J., Palm, D., & Helmreich, E. J. M. (1984b) *Biochemistry* (preceding paper in this issue).

Kokesh, F. C., & Kakuda, Y. (1977) *Biochemistry 16*, 2467–2473.

Konnert, J. H. (1976) *Acta Crystallogr., Sect. A A32*, 614–617.

Kossiakoff, A. A., & Spencer, S. A. (1980) *Nature (London) 288*, 414–416.

Lorek, A., Wilson, K. S., Sansom, M. S. P., Stuart, D. I., Stura, E. A., Jenkins, J. A., Zanotti, G., Hajdu, J., & Johnson, L. N. (1984) *Biochem. J. 218*, 45–60.

Madsen, N. B., & Withers, S. G. (1983) in *Chemical and Biological Aspects of Vitamin B_6 Catalysis* (Evangelopoulos, A. E., Ed.) pp 117–126, Liss, New York.

Makinen, M. W., & Fink, A. L. (1977) *Annu. Rev. Biophys. Bioeng. 6*, 301–343.

Parrish, R. F., Uhing, R. J., & Graves, D. J. (1977) *Biochemistry 16*, 4824–4831.

Pauling, L. (1946) *Chem. Eng. New 24*, 1375–1377.

Philip, G., Gringel, G., & Palm, D. (1982) *Biochemistry 21*, 3043–3050.

Rees, D. A., & Smith, P. J. C. (1975) *J. Chem. Soc.*, 838–840.

Sansom, M. S. P. (1983) D.Phil. Thesis, University of Oxford.

Sansom, M. S. P., Babu, Y. S., Hajdu, J., Stuart, D. I., Stura, E. A., & Johnson, L. N. (1983) in *Chemical and Biological Aspects of Vitamin B_6 Catalysis* (Evangelopoulos, A E., Ed.) pp 125–146, Liss, New York.

Shimomura, S., & Fukui, T. (1980) *Biochemistry 19*, 2287–2294.

Sotiroudis, T. G., Oikonomakos, N. G., & Evangelopoulos, A. E. (1978) *Eur. J. Biochem. 88*, 573–581.

Sprang, S. R., & Fletterick, R. J. (1979) *J. Mol. Biol. 131*, 523–551.

Sprang, S. R., Goldsmith, E. J., Fletterick, R. J., Withers, S. G., & Madsen, N. B. (1982) *Biochemistry 21*, 5364–5371.

Stuart, D. I., Levine, M., Muirhead, H., & Stammers, D. K. (1979) *J. Mol. Biol. 134*, 109–142.

Stura, E. A. (1981) D.Phil. Thesis, University of Oxford.

Stura, E. A., Zanotti, G., Babu, Y. S., Sansom, M. S. P., Stuart, D. I., Wilson, K. S., Johnson, L. N., & Van de Werve, G. (1983) *J. Mol. Biol. 170*, 529–565.

Takagi, M., Shimomura, S., & Fukui, T. (1981) *J. Biol. Chem. 256*, 728–730.

Takagi, M., Fukui, T., & Shimomura, S. (1982) *Proc. Natl. Acad. Sci. U.S.A. 79*, 3716–3719.

Titani, K., Koide, A., Hermann, J., Ericsson, L. H., Kumar, S., Wade, R. D., Walsh, K. A., Neurath, H., & Fischer, E. H. (1977) *Proc. Natl. Acad. Sci. U.S.A. 74*, 4762–4766.

Tu, J.-I., Jacobson, G. R., & Graves, D. J. (1971) *Biochemistry 10*, 1229–1236.

Weber, I. T., Johnson, L. N., Wilson, K. S., Yeates, D. G. R., Wild, D. L., & Jenkins, J. A. (1978) *Nature (London) 274*, 433–437.

Wilson, K. S., & Yeates, D. G. R. (1979) *Acta Crystallogr., Sect. A A35*, 146–157.

Wilson, K. S., Stura, E. A., Wild, D. L., Todd, R. J., Stuart, D. I., Babu, Y. S., Jenkins, J. A., Standing, T. S., Johnson, L. N., Fourme, R., Kahn, R., Gadet, A., Bartels, K. S., & Bartunik, H. D. (1983) *J. Appl. Crystallogr. 16*, 28–41.

Withers, S. G., Madsen, N. B., & Sykes, B. D. (1981a) *Biochemistry 20*, 1748–1756.

Withers, S. G., Madsen, N. B., Sykes, B. D., Takagi, M., Shimomura, S., & Fukui, T. (1981b) *J. Biol. Chem. 256*, 10759–19762.

Withers, S. G., Madsen, N. B., Sprang, S. R., & Fletterick, R. J. (1982a) *Biochemistry 21*, 5372–5382.

Withers, S. G., Madesen, N. B., & Sykes, B. D. (1982b) *Biochemistry 21*, 6716–6722.

Withers, S. G., Schechosky, S., & Madsen, N. B. (1982c) *Biochem. Biophys. Res. Commun. 108*, 322–329.

Wolfenden, R. (1969) *Nature (London) 223*, 704–705.